Conformational Features of the Full-Length HIV and SIV Nef Proteins Determined by Mass Spectrometry†

James M. Hochrein,‡ Thomas E. Wales,‡ Edwina C. Lerner,§ Anthony P. Schiavone,§ Thomas E. Smithgall,§ and John R. Engen*,‡

Department of Chemistry, University of New Mexico, Albuquerque, New Mexico 87131, and Department of Molecular Genetics and Biochemistry, University of Pittsburgh School of Medicine, Pittsburgh, Pennsylvania 15261

Received March 4, 2006; Revised Manuscript Received April 27, 2006

ABSTRACT: The Nef protein from human or simian immunodeficiency virus enhances viral replication, downregulates immune cell receptors, and activates multiple host cell signaling pathways. Conformational information about full-length Nef has been difficult to obtain as the full-length protein is not readily amenable to NMR or X-ray crystallography due to aggregation at high concentrations. As an alternative, full-length HIV and SIV Nef were probed with hydrogen exchange mass spectrometry, a method compatible with the low concentration requirements of Nef. The results showed that HIV Nef contains a solvent-protected core, as previously demonstrated with both NMR and X-ray crystallography. SIV Nef, for which there is no structural information, had a similar protected core, although it was more flexible and dynamic than its HIV counterpart. Many of the regions outside the core in both SIV and HIV Nef were highly solvent exposed. However, limited protection from exchange was observed in both N- and C-terminal regions, suggesting the presence of structured elements. Protection from exchange was also observed in a large loop emanating from the core that was deleted for NMR and X-ray analysis. These data show that while the majority of Nef was highly solvent exposed, regions outside the core may have structural attributes which may contribute to Nef functions known to map to these regions.

The Nef protein from human (HIV-1[1] and HIV-2) or simian (SIV) immunodeficiency virus enhances viral replication, downregulates immune cell receptors, activates multiple host cell signaling pathways, and is essential for high viral loads and progression to AIDS (reviewed in refs *1*−*6*). While the *nef* gene is conserved among all primate lentiviruses, SIV Nef appears to serve the same functional role as HIV Nef through a slightly different mechanism (*7*−*10*). SIV Nef binds the Hck tyrosine kinase via its SH2 domain rather than through the SH3 domain as in HIV Nef. Further, SIV Nef utilizes its first 50 amino acids for Hck interaction, while these residues in HIV Nef are not required for Hck binding.

Structural information about parts of HIV Nef has been produced by NMR (*11*, *12*) and X-ray crystallography (*13*, *14*). Full-length HIV Nef could not be crystallized, whereas a deletion variant including residues 54−205 (*13*) or 58−206 (*14*) provided crystals suitable for structural determination. However, residues 54−69 and 149−178 remained disordered in both crystals. As full-length HIV Nef was prone to aggregation and significant parts of HIV Nef were highly flexible in solution, residues 2−39 and 159−173 were removed for solution NMR structural work (*11*, *12*). The N-terminal region of HIV Nef (residues 1−25 and 2−57) was also investigated by NMR (*15*, *16*) and found to be mostly disordered. The structure of the N-terminal region seems to be dependent on myristoylation (*15*), and conformational changes have been observed upon myristoylation (*17*). All the known structural information for HIV Nef has been assembled into a model of the full-length protein (*18*). In the model, the conformation of the loop between residues 157 and 174 remains unknown, and the residues were inserted with a probable conformation before energy minimization. Figure 1A summarizes the regions of HIV Nef for which structural information has been obtained. There is currently no structural information for SIV Nef.

Nef is a multifunctional protein (*2*, *3*, *6*). Some of its key disease-related functions map to regions where Nef appears to be unstructured. For example, residues 62−65 in the N-terminal region of HIV Nef are required for MHC-I downregulation (*19*−*21*), and two residues in the large unstructured loop (D174 and D175) appear to be necessary for CD4 downregulation (*22*). It is important, therefore, not only to understand the conformation of the parts of Nef for which limited structural information has yet been obtained but also to have a method that can provide information about changes to the structure of these regions during Nef interactions with cellular partners that are important for disease progression.

To further future biophysical analyses of the interactions of Nef with binding partners and to elucidate the nature of

† Funded by grants from the NIH: R01-GM070590 (J.R.E.) and R01-AI57083 (T.E.S.).

* To whom correspondence should be addressed: Clark Hall 242, MSC03-2060, Department of Chemistry, University of New Mexico, Albuquerque, NM 87131. Telephone: (505) 277-4226. Fax: (505) 277-2609. E-mail: engen@unm.edu.

‡ University of New Mexico.

§ University of Pittsburgh School of Medicine.

[1] Abbreviations: HIV, human immunodeficiency virus; SIV, simian immunodeficiency virus; HXMS, hydrogen exchange mass spectrometry; PONDR, predictors of natural disordered regions.

10.1021/bi060438x CCC: $33.50
Published on Web 06/01/2006

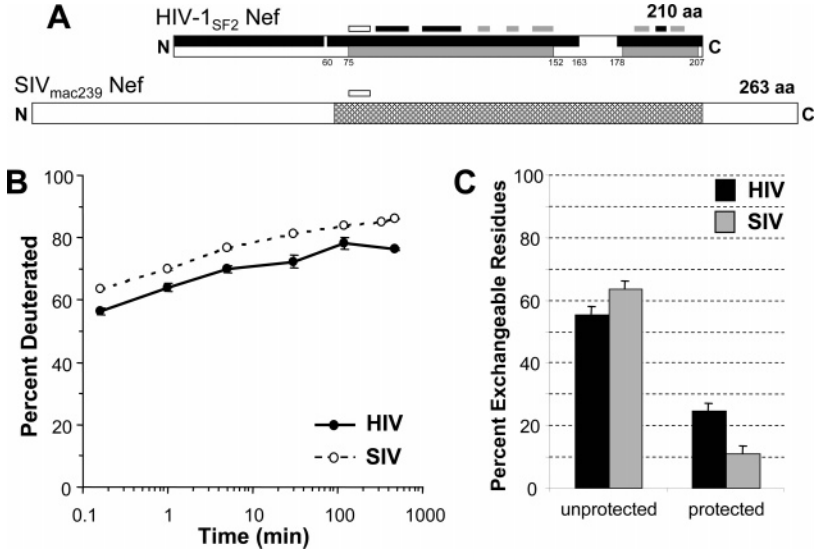

FIGURE 1: (A) Comparison of HIV and SIV Nef. The regions of HIV Nef for which there are X-ray crystallographic data are colored gray (PDB entries 1EFN and 1AVZ); regions where there is NMR structural information are colored black [residues 1−25, PDB entry 1ZEC; residues 2−57, PDB entry 1QA5; and residues 60−210,Δ163−177 in our numbering (which corresponds to residues 56−206,Δ159−172 in PDB entry 2NEF)]. Structural elements previously determined are shown on top of HIV Nef: white box, PPII domain; black lines, α helices; and gray lines, β strands. The shaded region of SIV Nef is predicted to be highly similar to the structured region of HIV Nef (*1*, *9*). (B) Hydrogen exchange into intact HIV (●) and SIV (○) Nef. The deuterium level has been adjusted assuming 12% back-exchange during analysis. The maximum deuteration levels for HIV and SIV Nef are 201 and 248, respectively. The error bars represent the range of two independent determinations. (C) Comparison of exposed and protected residues in intact HX in SIV and HIV Nef. Unprotected residues were defined as those that had exchanged already by the shortest time point used (10 s), while protected residues were those that did not exchange during the 8 h time course (the difference between the total number of exchangeable backbone amide hydrogens and the number that exchanged after 8 h, panel B).

the SIV Nef conformation relative to HIV Nef, we have used hydrogen exchange mass spectrometry (HXMS) to probe the conformation of HIV and SIV Nef. In contrast to all previous structural work with NMR, it was possible to analyze both full-length Nef proteins with HXMS at concentrations of <28 μM. Nef has a tendency to form higher-order multimers at the concentrations (≥200 μM) required for NMR, and the nonmyristoylated form (used here) has been reported to form multimers in solution (*23*). Our HXMS results demonstrate that some type of structure exists in the parts of Nef that have been deleted in previous structural investigations or deemed totally unstructured, suggest that the core of SIV Nef is similar to HIV Nef, and indicate that SIV Nef is more dynamic than its HIV Nef counterpart.

MATERIALS AND METHODS

Production of HIV and SIV Nef. Nef from either HIV-1 (SF2 strain) or SIV (mac293 strain) was amplified by PCR and subcloned into baculoviral transfer vector pVL1393 using the BamHI and EcoRI cloning sites. The cloning resulted in addition of a six-His tag (MHHHHHH) at the N-terminus followed by the second coding amino acid (glycine) for both HIV and SIV Nef. The resulting transfer vectors were used to produce recombinant baculoviruses in Sf-9 insect cells using Baculogold baculovirus DNA as described previously (*24*). To express six-His Nef (same procedure for either SIV or HIV Nef), Sf-9 insect cells were grown to a cell density of 1.5×10^6 cells/mL in 1 L of Graces supplemented insect medium (GIBCO) containing 10% FBS. One hundred milliliter of high-titer baculovirus was added to the culture medium. The infected cells were harvested 40−48 h post-infection by centrifugation and washed once in ice-cold PBS. The cell pellet was flash-frozen in liquid nitrogen and stored at −80 °C until purification. To purify six-His Nef, the cell pellet was thawed and sonicated in a buffer containing 20 mM Tris (pH 8.3), 500 mM NaCl, 5 mM β-mercaptoethanol, 20 mM imidazole, and 10% glycerol. The lysate was cleared by centrifugation and loaded onto a His-trap chelating column (Amersham, 5 mL) using FPLC (Bio-Rad). The six-His Nef was eluted with a linear imidazole gradient (from 20 mM to 1.0 M), and the fractions containing the six-His Nef protein were identified on an SDS−PAGE gel with Western blotting using an anti-His antibody (His probe H-15, Santa Cruz). The fractions containing six-His Nef were pooled and dialyzed in a buffer containing 20 mM Tris, 100 mM NaCl, and 3 mM DTT (pH 8.3). The concentration of purified six-His Nef was obtained using a scanning densitometer (Quantity One software, Bio-Rad) with BSA as the concentration control. The mass of each purified protein was verified with electrospray mass spectrometry (see Figure 1s of the Supporting Information).

Hydrogen Exchange. Deuterium labeling methods were similar to those previously described (*25*, *26*). Briefly, HIV and SIV Nef were independently incubated at 21 °C in 20 mM Tris, 100 mM NaCl, and 3 mM DTT (pH 8.3) for 10 min prior to labeling. Approximately 6 nmol of protein [at a concentration of 28 μM (HIV Nef) or 6.4 μM (SIV Nef)] was labeled by adding a 15-fold excess of 99% deuterium oxide in 20 mM Tris, 100 mM NaCl, and 3 mM DTT (pD 7.42). At various time points ranging from 10 s to 8 h, an aliquot (400 pmol) of labeled protein was removed, and 0.5 N HCl was used to reduce the pH to 2.50 and quench the labeling reaction.

Intact Protein Analysis. Full-length protein (HIV or SIV Nef) was analyzed immediately after the labeling reaction was quenched. Each quenched sample was injected onto a

1 mm × 8 mm protein trap (Michrom Biosciences) and desalted for 3 min at 2% acetonitrile at a flow rate of 100 μL/min. After desalting had been carried out, the acetonitrile concentration was increased to 98% to elute the protein. Both HPLC solvents contained 0.05% TFA, and all tubing and valves were placed in an ice bath to minimize deuterium back-exchange (*27*). The eluant was directed into a Waters QTOF2 for mass analysis. The parameters of the mass spectrometer were as follows: capillary voltage of 2.7 kV, cone voltage of 35 V, source temperature of 85 °C, desolvation temperature of 175 °C, and nitrogen gas flow of 500 L/h. The mass spectrometer was scanned over the *m*/*z* range of 50−1990 with a scan time of 2.4 s and an interscan time of 0.1 s. Each mass determination was calibrated with horse heart myoglobin infused at the end of the chromatographic run. The resulting mass spectra were converted from the *m*/*z* scale to molecular mass using the transform algorithm in MassLynx. The centroid of each mass for each labeled time point was determined. The difference in mass between the unlabeled control and each exchange time point was used to determine the extent of deuterium incorporation. A totally deuterated form of either HIV or SIV Nef could not be prepared. Both proteins (particularly SIV Nef) began to degrade after extended periods of time (>12 h) at elevated temperatures (>35 °C) or at low pH (DCl). A totally deuterated form could not be prepared with denaturants either as it proved extremely difficult to remove denaturants from the proteins prior to mass analysis. Therefore, the level of back-exchange (*27*) was estimated to be 12% (based on totally deuterated standard proteins), and all data were adjusted according to the method of ref *28*.

Peptic Peptide Analysis. On-line pepsin digestion was used to localize deuterium uptake. Labeled protein was prepared as described above and injected at a flow rate of 250 μL/min into a 2.1 mm × 50 mm stainless steel column (Alltech part 65175) packed with pepsin immobilized on POROS-20AL beads (PerSeptive Biosystems). Under these conditions, the digestion time was approximately 45 s. Immobilized pepsin was prepared according to the method of ref *29*. The resulting peptides were trapped on a 1 mm × 8 mm peptide trap (Michrom Biosciences) and desalted for 3 min. The peptides were eluted from the trap with a gradient of 2 to 98% acetonitrile in 10.5 min at a flow rate of 50 μL/min and separated with a Magic C-18, 5 μm 200 Å, 1.0 mm × 50 mm column (Michrom Biosciences). The same QTOF2 mass spectrometer was used for mass analysis with the same parameters as described above for the intact protein analysis. Peptides were identified and data processed by centroiding an isotopic distribution corresponding to the +2, +3, or +4 charge state of each peptide. The relative level of deuterium incorporation in each peptide was plotted as deuterium level versus the exchange time. This was repeated for both HIV and SIV Nef, and levels of deuterium uptake for overlapping regions were compared. All of the results were adjusted by 15% to account for back-exchange during analysis. The adjustment for back-exchange is an average value which is suitable for the majority of peptides. In a few cases (*27*), the correction is slightly more than necessary. Because a totally deuterated protein could not be prepared (see above), a few peptides are overcorrected (Figure 3).

To identify the peptic peptides, undeuterated intact full-length proteins were digested with the same pepsin column described above. The peptides were collected and injected onto a Ultimate Dionex LC system for reverse phase separation and spotting (Probot) to a MALDI plate. MS/MS was performed on each peptide in each spot with an Applied Biosystems 4700 MALDI to positively identify each peptic peptide. Peptic peptides covering >85% of HIV and SIV were identified (see Tables 1S and 2S of the Supporting Information).

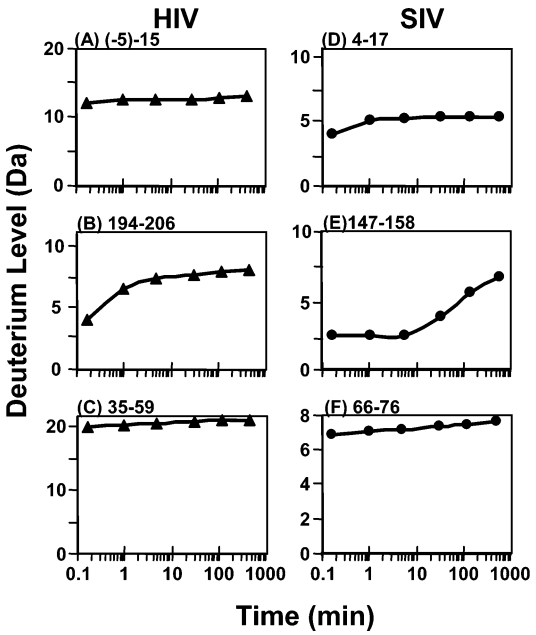

FIGURE 2: Deuterium uptake curves for selected regions of HIV (A−C) and SIV (D−F) Nef. Examples of the HXMS results for three peptic peptides in each protein are shown and correspond to the extreme N-terminal region (A and D), areas of known or predicted structure (B and E) (see Figure 1A), and the region just before the PPII helix (C and F). The deuterium level of each peptide has been adjusted assuming 15% back-exchange during analysis. The maximum of the *Y*-axis in each graph corresponds to the number of maximum exchangeable backbone amide hydrogens in each peptide (see also Tables 1S and 2S of the Supporting Information).

Calculations. Solvent accessibility calculations were made with WHAT IF (*30*) for each HIV Nef structure file in the Protein Data Bank (1AVZ, 1EFNB, 1EFND, and 2NEF model 1). The backbone accessibility values were tabulated in an Excel spreadsheet, and the average solvent accessibility for the backbone of each residue was calculated. No structural information for SIV Nef is available; hence, no calculations were made for SIV Nef. The PONDR (predictors of natural disordered regions) algorithm (*31*) with the standard parameter settings was used to calculate the amount of disorder for the HIV and SIV Nef sequences.

RESULTS AND DISCUSSION

Hydrogen Exchange. Hydrogen exchange mass spectrometry (HXMS) can be used to probe protein backbone dynamics and conformational changes (reviewed in refs *32*−*34*). Backbone amide hydrogens in proteins can undergo exchange with hydrogens in solution. The presence of structure (i.e., hydrogen bonding and protection from solvent) may reduce the rates of backbone amide hydrogen exchange by up to 10^8-fold over the rate observed for unstructured amino acid sequences (*32*). By measuring the level of incorporation of deuterium into proteins with mass spec-

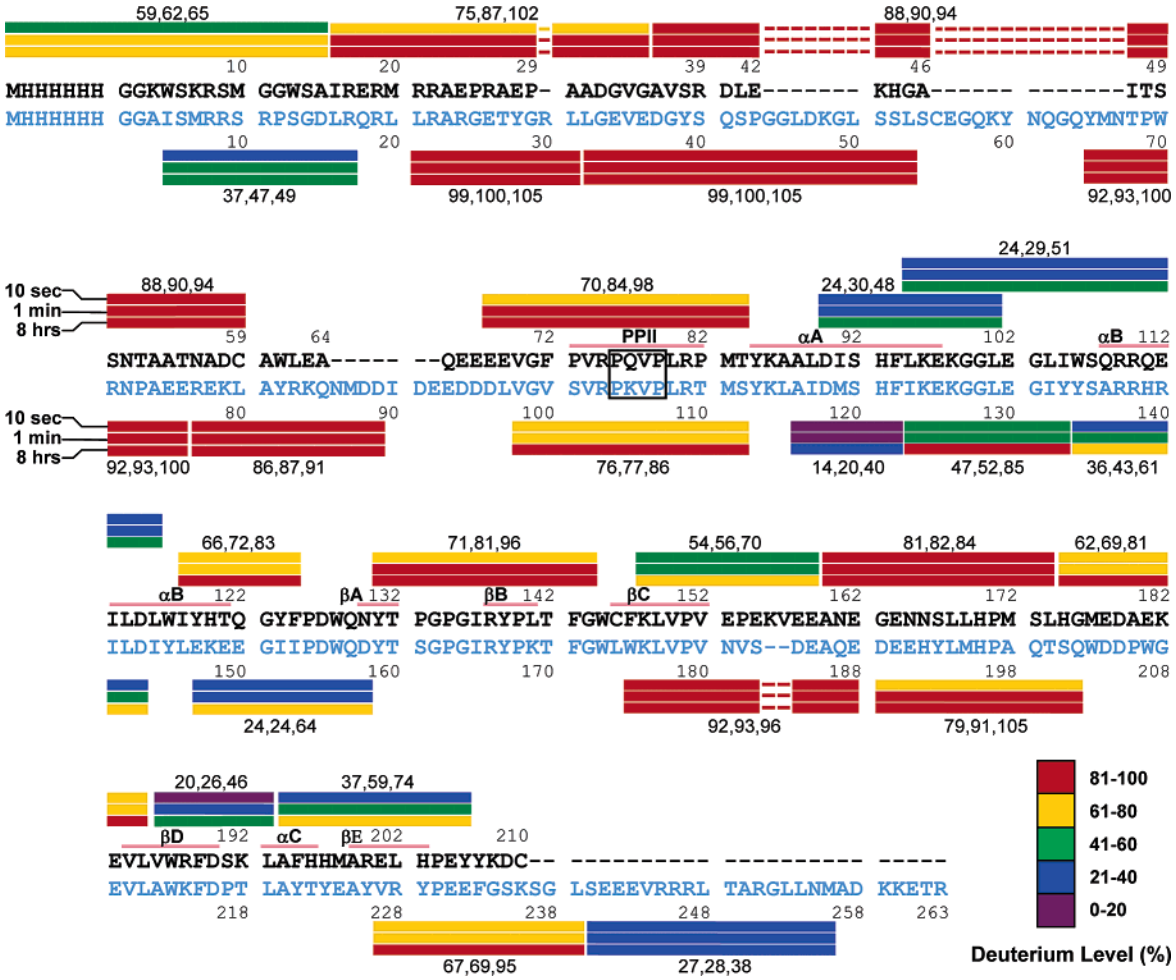

FIGURE 3: Summary of incorporation of deuterium into peptic peptides of HIV and SIV Nef. The sequence of both proteins is shown with HIV Nef at the top (black) and SIV Nef at the bottom (blue). The alignment was done on the basis of refs *9* and *15*. The numbering starts at the second amino acid of each Nef protein and does not include the six-His purification tag. Structural elements are indicated above the HIV Nef sequence. Each peptic peptide is shown as three colored bars either above (HIV Nef) or below (SIV Nef) the sequence. The deuteration level (%) is shown for three time points (10 s, top bar; 1 min, middle bar; and 8 h, bottom bar). The numbers above and below each peptide are the actual deuterium percentage for the three bars, from the shortest time point to the longest. All peptic peptides that were monitored are not shown (see also Tables 1S and 2S of the Supporting Information).

trometry, we can define regions of structure. Because hydrogen exchange rates are a function of both hydrogen bonding and solvent accessibility, it is not possible to determine the secondary structure in regions with reduced levels of exchange. It is, however, possible to delineate regions with structure from those that must be highly solvent exposed. Protein dynamics are also concurrently revealed.

Deuterium incorporation can be assessed for the full-length, intact protein; on the other hand, the labeled protein can be digested with an acid protease, and the deuterium levels of all the fragments were measured. By performing the digestion step, we can assess the deuterium incorporation in distinct regions. HXMS was used to probe the structural features of HIV and SIV Nef first for the intact, undigested proteins and then for peptic fragments that covered nearly all of the backbone for each protein.

Intact Protein Analysis. Deuterium uptake was assessed for full-length HIV and SIV Nef by incubating each protein in deuterium for various amounts of time. The mass increase was measured with electrospray mass spectrometry and was plotted as the percent deuterated (Figure 1B). SIV Nef incorporated slightly more deuterium than HIV Nef. The incorporation of deuterium at two distinct time points was compared (Figure 1C). The residues designated as unprotected were those that had exchanged by the first time point in the analysis (10 s). Backbone amide hydrogens that were highly solvent exposed and not hydrogen bonded would be expected to exchange very rapidly (*35*) and certainly would have exchanged after 10 s in D_2O at pH 7.0. According to this criteria, SIV Nef had ~57 more unprotected amide hydrogens than HIV Nef. As SIV Nef has 53 more residues than HIV Nef (which are predicted to be in unstructured, solvent-exposed loops), this result was not surprising. Protected residues were defined as those that had not exchanged after 8 h in deuterium (calculated by subtracting the deuterium level at 8 h from the total exchangeable backbone amide hydrogens in each protein). Defined in this way, protected residues report on the dynamics of the structured portion of the molecule and/or the highly protected region of the protein. The greater the movements and backbone dynamics, the fewer the number of residues that will be defined as protected. HIV Nef had approximately 15% more protected residues than SIV. This result implies that SIV Nef either is more dynamic in solution than HIV Nef, has a smaller highly exchange protected core, or both.

Peptide Analysis. To determine where deuterium incorporation is fast and slow, and therefore which regions of a protein are likely unstructured or structured, a protein can be labeled with deuterium and digested prior to mass analysis. Protein digestion in HXMS has been shown to be an effective method for gaining localized information about deuterium uptake (*27*). Because quench conditions must be maintained during the digestion, it is essential to use a protease with high activity at the quench pH of 2.5. Pepsin is ideal for such a digestion, but it cleaves nonspecifically. However, the digestion is reproducible under identical conditions. The identity of each peptic peptide from the digestion of HIV and SIV Nef was confirmed with exact mass or tandem MS experiments (Tables 1S and 2S of the Supporting Information).

Intact HIV and SIV Nef were labeled with D_2O; the exchange reaction was quenched, and the proteins were digested with pepsin. The incorporation of deuterium into each peptic peptide was assessed with electrospray mass spectrometry for peptides that represented >85% of the sequence of each protein. For HIV Nef, deuterium incorporation was followed for 15 peptides, while for SIV Nef, deuterium incorporation into 18 peptic peptides was assessed. Representative data for several peptides from HIV Nef and SIV Nef are shown in Figure 2. At the extreme N-terminus of both HIV and SIV Nef, there is some protection from exchange (Figure 2A,D). Some regions, such as those in known or predicted secondary structural elements (Figure 2B,E), indicate protection from deuterium exchange due to the presence of structure, while others (panels C and F) are almost completely deuterated by the earliest time point.

Exchange-in curves such as those in Figure 2 were obtained for all the peptic peptides from both proteins and were used to prepare a summary of the deuterium incorporation into both proteins (Figures 3 and 4). Figure 3 provides a comparison of the exchange in HIV Nef and SIV Nef, while Figure 4 indicates the levels of deuteration in HIV Nef peptic peptides (after 10 s and 8 h) on the model of full-length HIV Nef prepared by the method of ref *18*. In Figure 3, three time points at which to evaluate the deuterium levels were selected: 10 s, 1 min, and 8 h. For each time, the percentage of deuteration was calculated on the basis of the number of deuteriums that were incorporated and the total number of possible exchangeable hydrogens for that specific peptide. Bars representing the peptic peptides were color-coded to represent the percentage of deuteration for each of the three time points. Most of the regions of HIV Nef with known structure show significant protection from exchange. For example, in HIV Nef helicies A and B (peptides 90−104 and 95−116), the deuterium levels were between 48 and 51% after 8 h in deuterium, whereas in regions with no structure (such as peptide 68−84 in the PPII helix region), the deuterium level was 98% after 8 h of labeling. The complementary regions of structure in SIV Nef based on sequence alignments also show protection from exchange but become more deuterated by the final time points, consistent with SIV Nef being more dynamic as was shown with the intact protein results (Figure 1B,C). In the majority of the N-terminal region (residues 20−80, HIV Nef numbering) of both proteins, there was little or no protection from exchange, indicating that those regions were unstructured and highly exposed to solvent. At the very N-termini, there

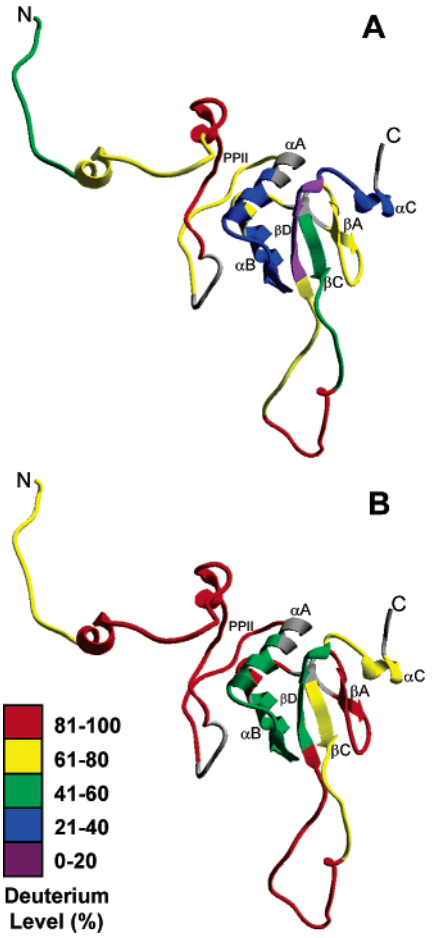

FIGURE 4: Deuterium incorporation results for HIV Nef from Figure 3 mapped onto the model of HIV Nef (*18*). Deuteration levels are shown after (A) 10 s and (B) 8 h in deuterium.

is some protection from exchange, implying that structure may exist in those areas. A small degree of protection was observed for the later part of the loop (residues 173−182, HIV Nef numbering). In the large loop between residues 163 and 178, there is again very rapid deuteration implying that little or no structure exists in those areas. The very C-terminal portion of SIV Nef also exhibited significant protection from exchange, again indicative of structure and/or protection from solvent.

The protection from exchange at the termini of SIV Nef and at the N-terminus of HIV Nef might be the result of formation of higher-order structures or aggregation in solution. At the concentrations used for the exchange reactions (28 μM), analytical gel filtration indicated that both HIV and SIV Nef were monomeric (data not shown). Although some structure exists in the N-terminal regions in the myristoylated form of HIV Nef (*15*), the protein analyzed here was not myristoylated.

Structural Predictions. The solvent accessibility of HIV Nef was calculated on the basis of the NMR and X-ray crystallographic data currently available for the core of the protein. Although there is NMR information for the ~60 N-terminal amino acids, no calculations were made for that portion of HIV Nef. The bars in Figure 5A represent the calculated backbone accessibility for each residue (see Materials and Methods for details). As expected, the accessibility correlated with the structural elements. The results of the hydrogen exchange determinations (Figure 3) were

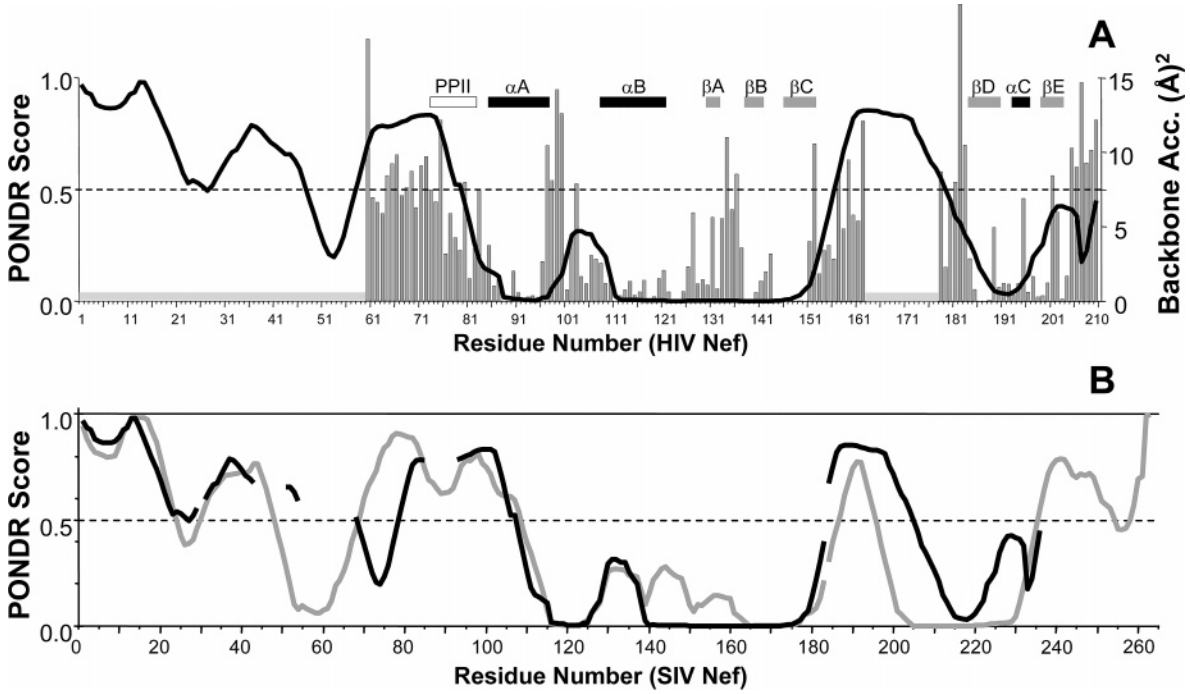

FIGURE 5: Solvent accessibility and prediction of disorder. (A) Solvent accessibility was calculated for each structure of HIV Nef (1AVZ, 1EFNB, 1EFND, and 2NEF model 1), averaged, and plotted vs residue number. Regions for which no structural data exist are indicated as a light gray bar at 0.5 Å^2. The PONDR score (see Materials and Methods) was calculated for HIV Nef and overlaid on the solvent accessibility graph as a solid black line. A dotted line indicates a PONDR score of 0.5. The known structural elements of HIV Nef are shown above the graph. (B) Comparison of the PONDR scores of HIV (black line, as in panel A) and SIV Nef (gray line). The residue numbering is for SIV Nef, and gaps are inserted in the appropriate places on the basis of the alignment of the two proteins (see Figure 3).

consistent with the accessibility calculations: in regions of significant protection, the exchange was slow, while in regions with predicted exposure, the exchange was rapid. The PONDR algorithm (*31*) was then used to predict which regions of HIV Nef are likely disordered and the resulting PONDR score overlaid on the accessibility calculations. The predictor is trained on both ordered and disordered sequences, and results are smoothed over a sliding window of nine amino acids. If a residue exceeds a threshold value of 0.5, then it is considered to be disordered. A PONDR score between 0.0 and 0.5 is consistent with order and structure. The PONDR prediction for HIV Nef was consistent with the accessibility calculations and the hydrogen exchange data. One exception was in the N-terminal region of HIV Nef in which the hydrogen exchange data indicated protection from exchange. The PONDR score in that region was near 1.0, predicting disorder. Overall, the hydrogen exchange data were consistent with the accessibility data, verifying the validity of the measurements. In addition, the PONDR prediction was generally correct and consistent with known structural information and hydrogen exchange results.

As there are no structural data for SIV Nef, the goal of the predictions in Figure 5A was to provide a baseline for the prediction of possible SIV Nef structure. The validity of the HXMS results and the PONDR predictions for HIV Nef make the SIV Nef predictions much more reliable. The PONDR scores were calculated for the sequence of SIV Nef and aligned with the PONDR prediction for HIV Nef (Figure 5B). In the core of Nef, the PONDR scores were similar for the two proteins, with PONDR predicting that the large loop in SIV Nef around residues 180−200 (SIV Nef numbering) is a bit smaller than the corresponding loop in HIV Nef. A region of structure in SIV Nef near residues 50−65 was also predicted by PONDR, and the N- and C-termini were not predicted to have much order. Otherwise, the two Nef proteins are highly similar according to the PONDR algorithm. The hydrogen exchange data (Figure 3) for SIV Nef are mostly consistent with the PONDR prediction. The region of structure predicted for SIV Nef around residues 50−65 did not appear to be protected from exchange, although the peptic peptide covering that exact sequence could not be found in the HXMS data. HXMS indicated protection from exchange in the C-terminus of SIV Nef, yet PONDR only predicted mild order in the region covering SIV Nef residues 250−260. Taken together, the results indicate that SIV Nef is highly similar to HIV Nef in its core region while its loops and N-termini are, like HIV Nef, mostly unstructured.

CONCLUSIONS

Full-length HIV and SIV Nef proteins were analyzed to gain information about the conformation and backbone dynamics of the regions absent in structural analyses. In this work, the first conformational investigation of SIV Nef, it was shown that SIV Nef is more dynamic in solution than HIV Nef. The N-terminal regions of both HIV and SIV Nef appear to have structure or are involved in some form of intra- or intermolecular interactions that lead to protection from exchange. As predicted for HIV Nef, the large loop near the middle of the protein is unstructured and solvent-exposed. HXMS verifies that the same is true for the corresponding loop in SIV Nef. The C-terminal regions of both HIV and SIV Nef also had some degree of protection from exchange.

The results of this study advance our understanding of Nef structure in several ways. First, they are in complete agreement with the model proposed for full-length HIV Nef

in ref *18*. Therefore, the use of this model is appropriate when dealing with the nonmyristoylated form of Nef. Similar HXMS studies are underway for the myristoylated form of HIV Nef in an attempt to elucidate any changes in structure compared with the nonmyristoylated form studied here. Second, these results lay the groundwork for future HXMS analyses of Nef in complex with other interacting proteins, particularly those that bind in the regions containing little or no structure. Changes to the hydrogen exchange profile upon protein−protein interactions will be indicative of protection, formation of structure, or both.

ACKNOWLEDGMENT

We thank Prof. Matthias Geyer for providing the coordinates for his HIV Nef model.

SUPPORTING INFORMATION AVAILABLE

Electrospray mass spectra of intact HIV New and SIV Nef (Figure 1s) and peptic peptides of HIV Nef (Table 1S) and SIV Nef (Table 2S). This material is available free of charge via the Internet at http://pubs.acs.org.

REFERENCES

1. Renkema, G. H., and Saksela, K. (2000) Interactions of HIV-1 NEF with cellular signal transducing proteins, *Front Biosci. 5*, D268−D283.
2. Geyer, M., Fackler, O. T., and Peterlin, B. M. (2001) Structure−function relationships in HIV-1 Nef, *EMBO Rep. 2*, 580−585.
3. Arold, S. T., and Baur, A. S. (2001) Dynamic Nef and Nef dynamics: How structure could explain the complex activities of this small HIV protein, *Trends Biochem. Sci. 26*, 356−363.
4. Fackler, O. T., and Baur, A. S. (2002) Live and let die: Nef functions beyond HIV replication, *Immunity 16*, 493−497.
5. Joseph, A. M., Kumar, M., and Mitra, D. (2005) Nef: "Necessary and enforcing factor" in HIV infection, *Curr. HIV Res. 3*, 87−94.
6. Baur, A. (2004) Functions of the HIV-1 Nef protein, *Curr. Drug Targets: Immune, Endocr. Metab. Disord. 4*, 309−313.
7. Greenway, A. L., Dutartre, H., Allen, K., McPhee, D. A., Olive, D., and Collette, Y. (1999) Simian immunodeficiency virus and human immunodeficiency virus type 1 nef proteins show distinct patterns and mechanisms of Src kinase activation, *J. Virol. 73*, 6152−6158.
8. Collette, Y., Arold, S., Picard, C., Janvier, K., Benichou, S., Benarous, R., Olive, D., and Dumas, C. (2000) HIV-2 and SIV nef proteins target different Src family SH3 domains than does HIV-1 Nef because of a triple amino acid substitution, *J. Biol. Chem. 275*, 4171−4176.
9. Shugars, D. C., Smith, M. S., Glueck, D. H., Nantermet, P. V., Seillier-Moiseiwitsch, F., and Swanstrom, R. (1993) Analysis of human immunodeficiency virus type 1 nef gene sequences present in vivo, *J. Virol. 67*, 4639−4650.
10. Carl, S., Iafrate, A. J., Lang, S. M., Stolte, N., Stahl-Hennig, C., Matz-Rensing, K., Fuchs, D., Skowronski, J., and Kirchhoff, F. (2000) Simian immunodeficiency virus containing mutations in N-terminal tyrosine residues and in the PxxP motif in Nef replicates efficiently in rhesus macaques, *J. Virol. 74*, 4155−4164.
11. Grzesiek, S., Bax, A., Clore, G. M., Gronenborn, A. M., Hu, J. S., Kaufman, J., Palmer, I., Stahl, S. J., and Wingfield, P. T. (1996) The solution structure of HIV-1 Nef reveals an unexpected fold and permits delineation of the binding surface for the SH3 domain of Hck tyrosine protein kinase, *Nat. Struct. Biol. 3*, 340−345.
12. Grzesiek, S., Bax, A., Hu, J. S., Kaufman, J., Palmer, I., Stahl, S. J., Tjandra, N., and Wingfield, P. T. (1997) Refined solution structure and backbone dynamics of HIV-1 Nef, *Protein Sci. 6*, 1248−1263.
13. Lee, C. H., Saksela, K., Mirza, U. A., Chait, B. T., and Kuriyan, J. (1996) Crystal structure of the conserved core of HIV-1 Nef complexed with a Src family SH3 domain, *Cell 85*, 931−942.
14. Arold, S., Franken, P., Strub, M. P., Hoh, F., Benichou, S., Benarous, R., and Dumas, C. (1997) The crystal structure of HIV-1 Nef protein bound to the Fyn kinase SH3 domain suggests a role for this complex in altered T cell receptor signaling, *Structure 5*, 1361−1372.
15. Geyer, M., Munte, C. E., Schorr, J., Kellner, R., and Kalbitzer, H. R. (1999) Structure of the anchor-domain of myristoylated and non-myristoylated HIV-1 Nef protein, *J. Mol. Biol. 289*, 123−138.
16. Barnham, K. J., Monks, S. A., Hinds, M. G., Azad, A. A., and Norton, R. S. (1997) Solution structure of a polypeptide from the N terminus of the HIV protein Nef, *Biochemistry 36*, 5970−5980.
17. Breuer, S., Gerlach, H., Kolaric, B., Urbanke, C., Opitz, N., and Geyer, M. (2006) Biochemical Indication for Myristoylation-Dependent Conformational Changes in HIV-1 Nef, *Biochemistry 45*, 2339−2349.
18. Geyer, M., and Peterlin, B. M. (2001) Domain assembly, surface accessibility and sequence conservation in full length HIV-1 Nef, *FEBS Lett. 496*, 91−95.
19. Mangasarian, A., Piguet, V., Wang, J. K., Chen, Y. L., and Trono, D. (1999) Nef-induced CD4 and major histocompatibility complex class I (MHC-I) down-regulation are governed by distinct determinants: N-Terminal α helix and proline repeat of Nef selectively regulate MHC-I trafficking, *J. Virol. 73*, 1964−1973.
20. Akari, H., Arold, S., Fukumori, T., Okazaki, T., Strebel, K., and Adachi, A. (2000) Nef-induced major histocompatibility complex class I down-regulation is functionally dissociated from its virion incorporation, enhancement of viral infectivity, and CD4 down-regulation, *J. Virol. 74*, 2907−2912.
21. Greenberg, M. E., Iafrate, A. J., and Skowronski, J. (1998) The SH3 domain-binding surface and an acidic motif in HIV-1 Nef regulate trafficking of class I MHC complexes, *EMBO J. 17*, 2777−2789.
22. Aiken, C., Krause, L., Chen, Y. L., and Trono, D. (1996) Mutational analysis of HIV-1 Nef: Identification of two mutants that are temperature-sensitive for CD4 downregulation, *Virology 217*, 293−300.
23. Dennis, C. A., Baron, A., Grossmann, J. G., Mazaleyrat, S., Harris, M., and Jaeger, J. (2005) Co-translational myristoylation alters the quaternary structure of HIV-1 Nef in solution, *Proteins 60*, 658−669.
24. Rogers, J. A., Read, R. D., Li, J., Peters, K. L., and Smithgall, T. E. (1996) Autophosphorylation of the Fes tyrosine kinase. Evidence for an intermolecular mechanism involving two kinase domain tyrosine residues, *J. Biol. Chem. 271*, 17519−17525.
25. Engen, J. R. (2003) Analysis of protein complexes with hydrogen exchange and mass spectrometry, *Analyst 128*, 3−8.
26. Engen, J. R., and Smith, D. L. (2000) Investigating the higher order structure of proteins. Hydrogen exchange, proteolytic fragmentation, and mass spectrometry, *Methods Mol. Biol. 146*, 95−112.
27. Zhang, Z., and Smith, D. L. (1993) Determination of amide hydrogen exchange by mass spectrometry: A new tool for protein structure elucidation, *Protein Sci. 2*, 522−531.
28. Hoofnagle, A. N., Resing, K. A., and Ahn, N. G. (2004) Practical methods for deuterium exchange/mass spectrometry, *Methods Mol. Biol. 250*, 283−298.
29. Wang, L., Pan, H., and Smith, D. L. (2002) Hydrogen exchange-mass spectrometry: Optimization of digestion conditions, *Mol. Cell. Proteomics 1*, 132−138.
30. Vriend, G. (1990) WHAT IF: A molecular modeling and drug design program, *J. Mol. Graphics 8*, 29, 52−56.
31. Li, X., Romero, P., Rani, M., Dunker, A. K., and Obradovic, Z. (1999) Predicting protein disorder for N-, C-, and internal regions, *Genome Inf. 10*, 30−40.
32. Smith, D. L., Deng, Y., and Zhang, Z. (1997) Probing the non-covalent structure of proteins by amide hydrogen exchange and mass spectrometry, *J. Mass Spectrom. 32*, 135−146.
33. Hoofnagle, A. N., Resing, K. A., and Ahn, N. G. (2003) Protein analysis by hydrogen exchange mass spectrometry, *Annu. Rev. Biophys. Biomol. Struct. 32*, 1−25.
34. Wales, T. E., and Engen, J. R. (2006) Hydrogen exchange mass spectrometry for the analysis of protein dynamics, *Mass Spectrom. Rev. 25*, 158−170.
35. Englander, S. W., and Kallenbach, N. R. (1983) Hydrogen exchange and structural dynamics of proteins and nucleic acids, *Q. Rev. Biophys. 16*, 521−655.

BI060438X